T. Ge
A. Y. T. Leung
*Department of Civil and Structural Engineering*
*University of Hong Kong*
*Pokfulam Road, Hong Kong*

# A Toeplitz Jacobian Matrix/Fast Fourier Transformation Method for Steady-State Analysis of Discontinuous Oscillators

*A semianalytical algorithm is proposed for the solutions and their stability of a piecewise nonlinear system. The conventional harmonic balance method is modified by the introduction of Toeplitz Jacobian matrices (TJM) and by the alternative applications of fast Fourier transformation (FFT) and its inverse. The TJM/FFT method substantially reduces the amount of computation and circumvents the necessary numerical differentiation for the Jacobian. An arc-length algorithm and a branch switching procedure are incorporated so that the secondary branches can be independently traced. Oscillators with piecewise nonlinear characteristics are taken as illustrative examples. Flip, fold, and Hopf bifurcations are of interest.* © *1995 John Wiley & Sons, Inc.*

## INTRODUCTION

Many physical systems exhibit complex nonlinearities that cannot be described by smooth analytical functions. Impacts and gaps are frequent examples in lubrication clearance, thermal expansion, manufacturing tolerances, and wears (Timoshenko et al., 1974; Nayfeh and Mook, 1979). The vibration of such systems includes the repeated smooth motions across the clearance space and impacts between the components. The equations of motion may be adequately represented by a piecewise-linear or more general, a piecewise-nonlinear system with sudden changes of stiffness and damping coefficients with respect to time. The resulting systems are, in most cases, strongly nonlinear with sophisticated dynamic behaviors (Shaw and Holmes, 1983; Thompson et al., 1983). Therefore, careful investigations must be carried out to avoid the unexpected behavior of discontinuities.

To this end, a number of techniques has been applied in the past by various researchers. The most direct methods for solving the strongly nonlinear vibration problems are the numerical time integration including the Runge–Kutta method, the Newmark method, etc. (e.g., Koh and Liaw, 1991). Although these methods provide both transient and steady-state responses for prescribed initial conditions, they require extremely

Received July 25, 1994; Accepted November 7, 1994.

Shock and Vibration, Vol. 2, No. 3, pp. 205–218 (1995)

CCC 1070-9622/95/030205-13

small time steps to avoid the divergence from the critical stability points and therefore result in tedious computations to reach a steady state. Their use is difficult in performing parameter studies, that is, to get frequency responses in a specified frequency range and to give multivalued solutions of the system at bifurcations. Analog simulation is frequently mentioned as a means of verification (e.g. Comparin and Singh, 1989). But this approach is closely dependent on the availability and the capacity of the analog computer and its equipped elements of nonlinearity. An analytical method to find the steady-state response of forced piecewise linear oscillators was proposed by Masri (1978) in which boundary values at the contact points are matched and the resulting nonlinear algebraic equations are then solved using Newtonian iteration. Further development of this method was reported by Bapat and Sankar (1986), Choi and Noah (1988, 1989), and Natsiavas (1989). Unfortunately, such computation involves the duration of contact which is extremely difficult to determine because the piecewise linear system is subjected to multiharmonic motions. Moreover, such a technique is restricted to piecewise linear systems. These methods will no longer be valid for nonlinear contact stiffnesses and impact dampers. On the other hand, Maezawa and Furukawa (1973) applied the harmonic balance method (HB) to analyze the symmetric and unsymmetric piecewise linear system. They represented the discontinuous stiffness function of a piecewise linear system by Fourier series and then solved the simultaneous equations for the Fourier iteratively. Lau et al. (1982) constructed the variational relationships between the time and the frequency domain and proposed an incremental harmonic balance method (IHB). The equivalence between the IHB and HBNR (harmonic balance with the Newton–Raphson iteration) methods was carefully proved by Ferri (1986). Both methods are energy conserving so that the stability information on the dynamic behavior can be acquired if an adequate number of terms is accommodated in the solution structure (Leung and Fung, 1989). The IHB method was applied to determine the periodic solutions of a friction-damped system and symmetric piecewise-linear stiffness systems by Pierre et al. (1985) and Lau and Zhang (1992), respectively. Choi and Noah (1988, 1989) and Kim and Noah (1991) modified the conventional harmonic balance using a fast Fourier transform (FFT) algorithm and studied the periodic system with an unsymmetric piecewise-linear stiffness, in which the responses and nonlinear forces were expressed by different discrete Fourier series. The relationship between the two series of expansions was associated by the FFT and the inverse FFT as well as the Newton–Raphson iteration. These recent extensions (named MIHB, the modified incremental method) made the conventional HB method more feasible for analyzing the general strongly nonlinear problem including the vibration of systems with piecewise-nonlinear characteristics. However, as pointed out by Ling and Wu (1987), the CPU time required by these methods increases exponentially with the number of harmonic terms even if the FFT algorithm has been utilized. This is because all of these methods need to execute double summations for each element of the Jacobian matrix in the Newton–Raphason iteration. Thus the calculation is only practical for a few harmonic terms (Lau and Zhang, 1992). Hence, the availability and accuracy of these approaches have been greatly limited by the computation cost and the capacity of computers. On the other hand, an alternative computation strategy to execute the harmonic balance was first reported by Ling and Wu (1987) in the fast Galerkin method (FG) and later by Cameron and Griffin (1989) in the alternating frequency/time method (AFT). Their procedures circumvent the tedious processing of the Jacobian Matrix by means of numerical differentiation and substantially accelerate the iteration performance. In the vicinity of bifurcation points, however, these methods will lose their numerical stability so that they can neither accurately determine the location of the bifurcation point nor pursue the further postbifurcation analysis.

The objective of this article is to develop an efficient methodology that can be used to accurately predict the complicated dynamic behavior of a general piecewise-nonlinear system, based on the theory of Galerkin averaging (Urabe, 1965) and the discrete Fourier transformation (Brigham, 1974). We first simplify the complex formulation of the Jacobian matrix in terms of Toeplitz matrices that are matrices defined by a few vectors [see Eq. (19)]. These Toeplitz Jacobian matrices (TJM) are determined by an FFT algorithm from the damping coefficient and stiffness coefficient functions. Then we translate the TJM formulation from complex number to real one for computational efficiency. We incorporate an arc-length method into the proposed approach

to ensure the effectiveness and robustness of the algorithm in the neighborhood of critical stability points. A branch switching technique is also introduced to trace the secondary branches. Floquet eigenvalues can be found naturally from the variational equation of our method, which provides us the valuable stability information of the given solution. Finally, to illustrate the usefulness of our TJM/FFT method, the steady-state frequency response of a general piecewise-nonlinear system is analyzed. The complicated dynamic behavior including fold bifurcation, flip bifurcation, and Hopf bifurcation are observed in our study.

## GOVERNING EQUATIONS

Consider the single degree-of-freedom (DOF) piecewise-nonlinear system as shown in Fig. 1. The motion of the system is bounded on the right side due to the resistance of the hard spring. The nondimensional equation of motion for this system can be expressed as

$$x'' + c(x)x' + g(x) = e(t), \tag{1}$$

where the prime represents derivative with respect to time $t$, $c(x)$ is a positive piecewise smooth damping function,

$$c(x) = \begin{cases} c_1 + c_2, & x > x_s \\ c_1, & x \le x_s \end{cases}, \tag{2}$$

and $g(x)$ is a piecewise-nonlinear restoring force (Fig. 2)

$$g(x) = \begin{cases} k_1 x + k_2(x - x_s)^3, & x > x_s \\ k_1 x, & x \le x_s \end{cases}. \tag{3}$$

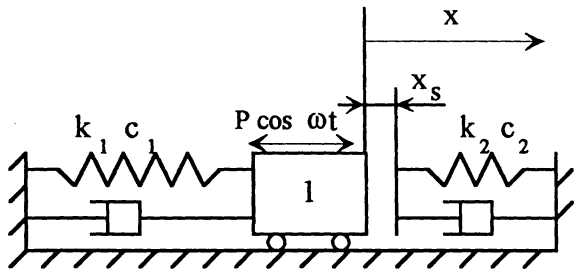


**FIGURE 1** Piecewise-nonlinear system.

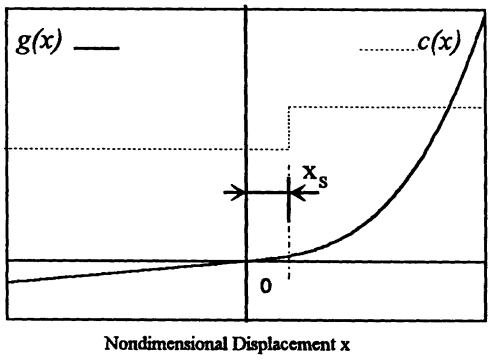


**FIGURE 2** Piecewise-nonlinear system.

In this study, the right-hand forcing $e(t)$ is simply a sinusoidal function

$$e(t) = P\cos(\omega t). \tag{4}$$

Here $P$ is assumed to be constant if frequency responses are of interest. For computation convenience, we further introduce a nondimensional time factor $\tau$ given by $\tau = \omega t$, and a function $f(\cdot)$ to represent the state of Eq. (1),

$$f(x, \dot{x}, \ddot{x}, \omega, \tau) = \omega^2\ddot{x} + \omega c(x)\dot{x} + g(x) - P\cos\tau = 0, \tag{5}$$

where the overdot denotes derivatives with respect to $\tau$.

## FORMULATION OF TJM/FFT METHOD

If one takes a small perturbation to the system equation,

$$\begin{Bmatrix} x \\ \dot{x} \\ \ddot{x} \\ \omega \end{Bmatrix} = \begin{Bmatrix} x_0 \\ \dot{x}_0 \\ \ddot{x}_0 \\ \omega_0 \end{Bmatrix} + \begin{Bmatrix} \Delta x \\ \Delta\dot{x} \\ \Delta\ddot{x} \\ \Delta\omega \end{Bmatrix}. \tag{6}$$

The corresponding state function $f(\cdot)$ can be approximated by

$$f(x_0 + \Delta x, \dot{x}_0 + \Delta\dot{x}, \ddot{x}_0 + \Delta\ddot{x}, \omega_0 + \Delta\omega, \tau) = f(x_0, \dot{x}_0, \ddot{x}_0, \omega_0, \tau_0) + \left.\frac{\partial f}{\partial \ddot{x}}\right|_0 \Delta\ddot{x} + \left.\frac{\partial f}{\partial \dot{x}}\right|_0 \Delta\dot{x} + \left.\frac{\partial f}{\partial x}\right|_0 \Delta x + \left.\frac{\partial f}{\partial \omega}\right|_0 \Delta\omega + \text{HOT} = 0, \tag{7}$$

where HOT represents the higher order terms.

The variational equation dependent on time $\tau$ is

$$f(\tau) = \omega_0^2 \Delta\ddot{x} + \omega_0 \alpha(x_0)\Delta\dot{x} + \beta(x_0)\Delta x - r(\tau) = 0, \tag{8}$$

or as a linear homogeneous equation,

$$\omega_0^2 \Delta\ddot{x} + \omega_0 \alpha(x_0)\Delta\dot{x} + \beta(x_0)\Delta x = r(\tau), \tag{9}$$

where $\alpha(x)$ is the unit step damping function,

$$\alpha(x) = \frac{\partial[c(x)\dot{x}]}{\partial\dot{x}} = \begin{cases} c_2, & x > x_s \\ \dfrac{c_1 + c_2}{2}, & x = x_s. \\ c_1 & x < x_s \end{cases} \tag{10}$$

$\beta(x)$ is the tangent stiffness function,

$$\beta(x) = \frac{\partial g(x)}{\partial x} = \begin{cases} k_1 + 3k_2(x - x_s)^2, & x > x_s \\ k_1 & x \le x_s \end{cases}. \tag{11}$$

Clearly, $\alpha(x)$, $\beta(x)$ are the synchronizing functions of the displacements. For the convenience of time discretization, we indicate $\alpha(x_0)$, $\beta(x_0)$ more explicitly as the form of time dependent functions $\alpha(\tau)$, $\beta(\tau)$. The term $r(\tau)$, on the right side of (9), is the residual function that can be used as a predictor when an accurate equilibrium is given or a corrector when an approximated equilibrium configuration is given,

$$r(\tau) = \begin{cases} -[2\omega_0\ddot{x}_0 + \alpha(x_0)]\Delta\omega & \text{predictor} \\ -f(x_0, \dot{x}_0, \ddot{x}_0, \omega_0, \tau) & \text{corrector} \end{cases}. \tag{12}$$

In periodic vibration, one can expand the response and its increment as well as the residual function in a finite Fourier series

$$\begin{Bmatrix} x(\tau) \\ \Delta x(\tau) \\ f(\tau) \\ r(\tau) \end{Bmatrix} = \sum_{j=-N}^{N} \begin{Bmatrix} X_j \\ \Delta X_j \\ F_j \\ R_j \end{Bmatrix} \exp(\mathbf{i}j\tau), \tag{13}$$

where $\mathbf{i} = \sqrt{-1}$. Here the integer $N$ is the total number of harmonic terms included in the solution which is large enough to admit the ultimate harmonics occurring in the system. Similarly, to the synchronizing functions $\alpha(\tau)$, $\beta(\tau)$, we also have

$$\begin{Bmatrix} \alpha(\tau) \\ \beta(t) \end{Bmatrix} = \sum_{j=-N}^{N} \begin{Bmatrix} A_j \\ B_j \end{Bmatrix} \exp(\mathbf{i}j\tau), \tag{14}$$

where $A_j$ and $B_j$ are the harmonic components of the time function $\alpha(\tau)$, $\beta(\tau)$. Particularly, in the case of linear vibration ($x_{\max} \le x_s$), one has

$$\begin{cases} A_j = c_1, & B_j = k_1 \quad j = 0 \\ A_j = B_j = 0 & \text{otherwise} \end{cases}.$$

Substitution of (13) into (6) leads to

$$f(\tau) = \sum_{j=-N}^{N} [\beta(\tau) - j^2\omega_0^2 + \mathbf{i}j\omega_0\alpha(\tau)]\Delta X_j \exp(\mathbf{i}j\tau) - r(\tau). \tag{15}$$

The next step is to sample the oscillator period with $M$ interval-equivalent discrete points. According to the sampling theorem, the maximum number of points $M$ must be larger than or equal to $2N + 1$ to avoid the *aliasing distortion* in the resulting harmonic components. Under the time discretization, Eq. (15) becomes

$$f\left(\frac{2\pi q}{M}\right) = \sum_{j=-N}^{N}\left[\beta\left(\frac{2\pi q}{M}\right) - j^2\omega_0^2 + \mathbf{i}j\omega_0\alpha\left(\frac{2\pi q}{M}\right)\right]\Delta X_j \exp\left(\mathbf{i}\frac{2\pi qj}{M}\right) - r\left(\frac{2\pi q}{M}\right) = 0, \tag{16}$$

$$q \in \mathbf{N}[0, M - 1]$$

After applying the inverse discrete Fourier transformation to (16), one obtains the following periodic equations,

$$F_k = \sum_{q=0}^{M-1} \sum_{j=-N}^{N} \left[ \beta\left(\frac{2\pi q}{M}\right) - j^2\omega_0^2 + \mathbf{i}j\omega_0\alpha\left(\frac{2\pi q}{M}\right) \right] \Delta X_j \exp\left[\mathbf{i}\frac{-2\pi q(k-j)}{M}\right]$$
$$- \sum_{q=0}^{M-1} r\left(\frac{2\pi q}{M}\right)\exp\left(\mathbf{i}\frac{-2\pi qk}{M}\right) = 0 \tag{17}$$

$$k \in \mathbf{N}[-N, N], \quad q \in \mathbf{N}[0, M-1].$$

Further manipulation is to exchange the order of the inner and outer summations in Eq. (17) and to put them into matrix form in terms of notation of the unknown incremental $\{\Delta\mathbf{X}\}$,

$$[\mathbf{J}]\{\Delta\mathbf{X}\} = \{\mathbf{R}\}, \tag{18}$$

where,

$$\{\Delta\mathbf{X}\} = [\Delta X_{-N}, \Delta X_{-N+1}, \ldots, \Delta X_0, \ldots, \Delta X_{N-1}, \Delta X_N]^T,$$
$$\{\mathbf{R}\} = [R_{-N}, R_{-N+1}, \ldots, R_0, \ldots, R_{N-1}, R_N]^T,$$

$[\mathbf{J}]$ is the Jacobian matrix used in the *Newton–Raphson* iteration, whose components are given by

$$J_{kj} = \frac{\partial F_k}{\partial X_j} = B_{k-j} - j^2\omega_0^2\delta_{k-j} + \mathbf{i}j\omega_0 A_{k-j} \tag{19}$$

in which $j$, $k$ denote the row and column location of the element in the Jacobian matrix $[\mathbf{J}]$. $\delta$ is the Kronecker function

$$\delta_{k-j} = \begin{cases} 1 & \text{if } k = j \\ 0 & \text{otherwise} \end{cases}. \tag{20}$$

$A_{k-j}$ and $B_{k-j}$ are the components of the *Toeplitz* matrices $[\mathbf{A}]$ and $[\mathbf{B}]$ that can be evaluated from the FFTs of the synchronizing functions $\alpha$ and $\beta$, respectively,

$$A_1 = \frac{1}{M}\sum_{q=0}^{M-1} \alpha\left(\frac{2\pi q}{M}\right)\exp\left(\frac{-\mathbf{i}2\pi qi}{M}\right) \tag{21}$$

$$B_1 = \frac{1}{M}\sum_{q=0}^{M-1} \beta\left(\frac{2\pi q}{M}\right)\exp\left(\frac{-\mathbf{i}2\pi qi}{M}\right), \tag{22}$$

where $i$ denotes the index of the convolution sequences used by the Toeplitz matrices, $i = k - j$. Because $\alpha$ and $\beta$ are evaluated at the $M$ discrete points in one period, the components of Toeplitz matrices $[\mathbf{A}]$ and $[\mathbf{B}]$ can be explicitly determined by using the IFFT technique. In case the index $i$ exceeds the dominant range $i \in \mathbf{N}[0, M-1]$, their values can also be found from the existing values of sequences by shifting the period over the $M$ points,

$$i = \mathrm{mod}\left(\frac{M + k - j}{M}\right). \tag{23}$$

Thus, once $A_i$, $B_i$ are found by FFTs from (21) and (22), the whole Jacobian matrix is determined. The resultant linear algebraic equation, Eq. (18), can be solved by any standard solver. The resulting solution is used to improve the original approximation. The updated harmonic response is transformed back into the time domain to update the damping function $\alpha(x)$, the stiffness function $\beta(x)$, and the corrector residual function $r$. An existing textbook procedure (Brigham, 1974) can be utilized to perform these two real Fourier transformations within one complex FFT algorithm. A flow chart that shows the complete iterative process of obtaining the steady-state periodic response is given in Fig. 3. In the AFT method (Cameron and Griffin, 1989) and the MIHB method (Kim and Noah, 1991), the number of points on time domain $M$ is equal to $2N + 1$ so that the harmonic components and the period discrete points are collocated giving the most efficient performance on switching back and forth between the frequency and time domains for continuous functions. However, in the present study, we include more discrete points $M$ to predict accurate locations of the turning point of the discontinuous functions and to increase the flexibility of using the efficient index 2 algorithms of FFT. The cost for such performance is

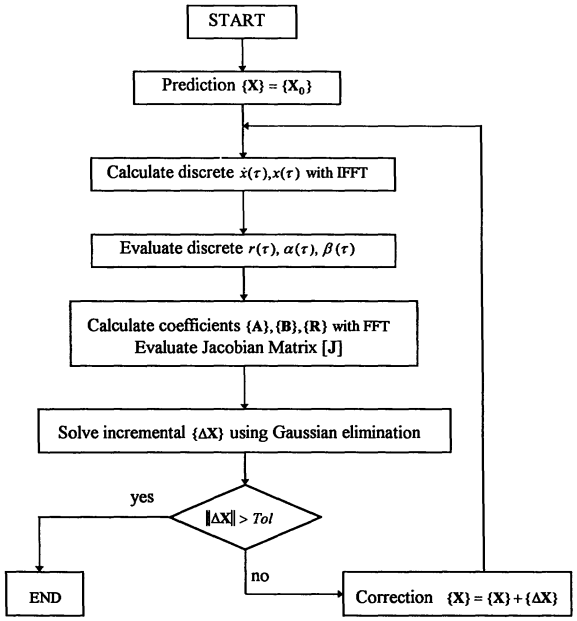


**FIGURE 3** Flow chart for TJM/FFT method.

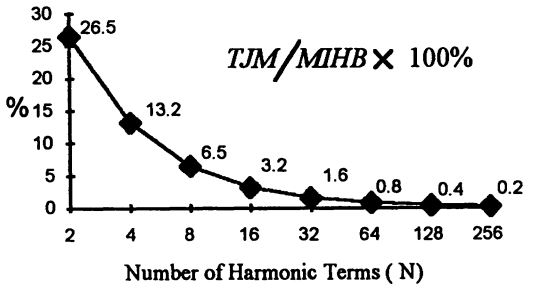


**FIGURE 4** Comparison of CPU times.

reasonable because the computation involved in the evaluation of the time functions at $M$ points is small compared to that in solving the harmonic increments.

The main advantage of this method in comparison with that used by Kim and Noah (1991) is the efficiency. The use of the TJM and FFT (TJM/FFT) greatly reduces the amount of the multiplication operations included in the MIHB and improves the numerical accuracy as well. The percentage of reduction of operation is demonstrated in Fig. 4.

## PROPOSED SCHEME FOR COMPUTER APPLICATION

### A Transformation for Real Jacobian Matrix

It is also advantageous to perform the TJM analysis in the real domain, because only $(2N + 1)$ real variables, instead of $(2N + 1)$ complex variables are required. Such reduction is possible due to the fact that components $X_j$ and $X_{-j}$ in (13) are complex conjugates. Assuming the original state function in Eq. (8) be expanded simultaneously by a real discrete Fourier series, one has

$$\begin{Bmatrix} x_q \\ \Delta x_q \\ f_q \\ r_q \end{Bmatrix} = \frac{1}{2}\begin{Bmatrix} U_0 \\ \Delta U_0 \\ C_0 \\ S_0 \end{Bmatrix} + \sum_{j=1}^{N} \begin{Bmatrix} U_j \\ \Delta U_j \\ C_j \\ S_j \end{Bmatrix} \cos\left(\frac{2\pi qj}{M}\right) + \begin{Bmatrix} V_j \\ \Delta V_j \\ D_j \\ W_j \end{Bmatrix} \sin\left(\frac{2\pi qj}{M}\right), \tag{24}$$

$$q \in \mathbf{N}[0, M].$$

Using (13), (24), and the identity $\exp(\mathbf{i}\theta) = \cos\theta + \mathbf{i}\sin\theta$, one has

$$\begin{cases} C_j = F_j + F_{-j} \\ D_j = \mathbf{i}(F_j - F_{-j}) \end{cases}, \quad \begin{cases} X_j = \frac{1}{2}(U_j - \mathbf{i}V_j) \\ X_{-j} = \frac{1}{2}(U_j + \mathbf{i}V_j) \end{cases}, \quad \text{and} \quad \begin{cases} S_j = R_j + R_{-j} \\ W_j = \mathbf{i}(R_j - R_{-j}) \end{cases}. \tag{25}$$

The resulting real form simultaneous equation can be written as

$$\begin{bmatrix} \mathbf{K}^{11} & \mathbf{K}^{12} \\ \mathbf{K}^{21} & \mathbf{K}^{22} \end{bmatrix} \begin{Bmatrix} \Delta \mathbf{U} \\ \Delta \mathbf{V} \end{Bmatrix} = \begin{Bmatrix} \mathbf{S} \\ \mathbf{W} \end{Bmatrix}, \tag{26}$$

where

$$\{\Delta\mathbf{U}\} = \{\Delta U_0, \Delta U_1, \ldots, \Delta U_N\}^T,$$
$$\{\Delta\mathbf{V}\} = \{\Delta V_1, \ldots, \Delta V_N\}^T$$
$$\{\mathbf{S}\} = \{S_0, S_1, \ldots, S_N\}^T,$$
$$\{\mathbf{W}\} = \{W_1, \ldots, W_N\}^T.$$

With the application of (25), the elements of the real Jacobian matrix $[\mathbf{K}^{ij}]$ can be found by the chain rule of differentiation,

$$\begin{aligned} K_{kj}^{11} = \frac{\partial C_k}{\partial U_j} &= \frac{\partial C_k}{\partial F_k}\frac{\partial F_k}{\partial X_j}\frac{\partial X_j}{\partial U_j} + \frac{\partial C_k}{\partial F_k}\frac{\partial F_k}{\partial X_{-j}}\frac{\partial X_{-j}}{\partial U_{-j}} \\ &+ \frac{\partial C_k}{\partial F_{-k}}\frac{\partial F_{-k}}{\partial X_j}\frac{\partial X_j}{\partial U_j} + \frac{\partial C_k}{\partial F_{-k}}\frac{\partial F_{-k}}{\partial X_{-j}}\frac{\partial X_{-j}}{\partial U_{-j}} \\ &= \frac{1}{2}[J_{k,j} + J_{k,-j} + J_{-k,j} + J_{-k,-j}] \\ &k \in \mathbf{N}[0, N], \quad j \in \mathbf{N}[0, N]. \end{aligned} \tag{27}$$

Similarly,

$$K_{kj}^{12} = \frac{\partial C_k}{\partial V_j} = \frac{\mathbf{i}}{2}[-J_{k,j} + J_{k,-j} - J_{-k,j} + J_{-k,-j}]$$
$$k \in \mathbf{N}[0, N], \quad j \in \mathbf{N}[1, N]$$
$$K_{kj}^{21} = \frac{\partial D_k}{\partial U_j} = \frac{\mathbf{i}}{2}[J_{k,j} + J_{k,-j} - J_{-k,j} - J_{-k,-j}]$$
$$k \in \mathbf{N}[1, N], \quad j \in \mathbf{N}[0, N]$$
$$K_{kj}^{22} = \frac{\partial D_k}{\partial V_j} = \frac{1}{2}[J_{k,j} - J_{k,-j} - J_{-k,j} + J_{-k,-j}]$$
$$k \in \mathbf{N}[1, N], \quad j \in \mathbf{N}[1, N].$$

In summary, an explicit transformation for the Jacobian matrix can be written as

$$\begin{Bmatrix} K_{kj}^{11} \\ K_{kj}^{12} \\ K_{kj}^{21} \\ K_{kj}^{22} \end{Bmatrix} = \frac{1}{2}\begin{bmatrix} 1 & 1 & 1 & 1 \\ -\mathbf{i} & \mathbf{i} & -\mathbf{i} & \mathbf{i} \\ \mathbf{i} & \mathbf{i} & -\mathbf{i} & -\mathbf{i} \\ 1 & -1 & -1 & 1 \end{bmatrix}\begin{Bmatrix} J_{k,j} \\ J_{k,-j} \\ J_{-k,j} \\ J_{-k,-j} \end{Bmatrix}. \tag{28}$$

## Arc-Length Method

In performing the parametric study along the equilibrium path of a nonlinear system, some geometric complications such as cusps, loops, and folds are frequently encountered due to the influence of nonlinear functions. The conventional iteration methods no longer converge because of the associated singularity. Therefore, to reveal the complicated characteristics of nonlinear response, it is necessary to introduce an auxiliary surface into the iteration scheme to enhance the robustness of the computation. The theory and applications of using the auxiliary surface have been widely discussed in the nonlinear finite element method or so-called *arc-length methods* (Crisfield, 1991). Among others, an adaptive arc-length parameterization scheme proposed by Riks (1984) is implemented in our study. Suppose one advances the solution curve with a prescribed step value $\rho$, the auxiliary spherical surface of radius $\rho$ will travel in an enlarged space $\mathbf{R}^{2N+2}$ and if there are intersections with the solution curves contained in original Eq. (8) the moving spherical surface will generate a sequence of points along these curves. The equation of the auxiliary surface is usually expressed as an arc-length constraint

$$\Psi(\mathbf{U}, \mathbf{V}, \omega) = 0. \tag{29}$$

Here $\rho$ is the prescribed arc length of the solution curve and $\Psi(\mathbf{U}, \mathbf{V}, \omega)$ takes the role of path functions that may be described by

$$\Psi(\mathbf{U}, \mathbf{V}, \omega) = \left[\frac{\partial \mathbf{U}}{\partial \rho}\right]^T\{\Delta\mathbf{U}\} + \left[\frac{\partial \mathbf{V}}{\partial \rho}\right]^T\{\Delta\mathbf{V}\} + \left(\frac{\partial \omega}{\partial \rho}\right)\Delta\omega, \tag{30}$$

where $\Delta\omega$ can be used as an active increment to obtain the frequency response of the system. On the other hand, the predictor and corrector in (12) are combined,

$$\begin{aligned} r(\tau) = &-[2\omega_0\ddot{x}_0 + \alpha(x_0)]\Delta\omega \\ &- f(x_0, \dot{x}_0, \ddot{x}_0, \omega_0, \tau). \end{aligned} \tag{31}$$

If $\alpha$ can be expanded by a real discrete Fourier series, one obtains

$$\alpha_q = \frac{G_0}{2} + \sum_{j=1}^{N} G_j \cos\left(\frac{2\pi qj}{M}\right) + H_j \sin\left(\frac{2\pi qj}{M}\right)$$
$$q \in \mathbf{N}[0, M], \tag{32}$$

where $G_j = A_j + A_{-j}$, $H_j = \mathbf{i}(A_j - A_{-j})$, and $A_j$ is given by Eq. (21).

The incremental equation, Eq. (27), becomes

$$\begin{bmatrix} \mathbf{K}^{11} & \mathbf{K}^{12} \\ \mathbf{K}^{21} & \mathbf{K}^{22} \end{bmatrix} \begin{Bmatrix} \Delta\mathbf{U} \\ \Delta\mathbf{V} \end{Bmatrix} = -\begin{Bmatrix} \mathbf{G} - 2\omega_0\mathbf{U} \\ \mathbf{H} - 2\omega_0\mathbf{V} \end{Bmatrix}_0 \Delta\omega - \begin{Bmatrix} \mathbf{C} \\ \mathbf{D} \end{Bmatrix}_0, \tag{33}$$

where subscript zero represents values given at the former iterating step and

$$\{\mathbf{U}\} = \{U_0, U_1, \ldots, U_N\}^T, \quad \{\mathbf{V}\} = \{V_1, \ldots, V_N\}^T,$$
$$\{\mathbf{C}\} = \{C_0, C_1, \ldots, C_N\}^T, \quad \{\mathbf{D}\} = \{D_1, \ldots, D_N\}^T,$$
$$\{\mathbf{G}\} = \{G_0, G_1, \ldots, G_N\}^T, \quad \{\mathbf{H}\} = \{H_1, \ldots, H_N\}^T,$$

Together with Eq. (30), one obtains the extended set of equations

$$\begin{bmatrix} \mathbf{K}^{11} & \mathbf{K}^{12} & (2\omega_0\mathbf{U}_0 - \mathbf{G}_0) \\ \mathbf{K}^{21} & \mathbf{K}^{22} & (2\omega_0\mathbf{V}_0 - \mathbf{H}_0) \\ \dfrac{\partial\mathbf{U}}{\partial\rho} & \dfrac{\partial\mathbf{V}}{\partial\rho} & \dfrac{\partial\omega}{\partial\rho} \end{bmatrix} \begin{Bmatrix} \Delta\mathbf{U} \\ \Delta\mathbf{V} \\ \delta\omega \end{Bmatrix} = -\begin{Bmatrix} \mathbf{C} \\ \mathbf{D} \\ \Psi - \rho \end{Bmatrix}_0 \tag{34}$$

in which $\Psi - \rho$ defines the searching direction on the solution curve along which the approximation errors are minimized.

The searching for bifurcation points and the calculation of secondary branches require additional consideration. In static nonlinear analysis, the location of bifurcation points and the exchange of stability of solutions for fold and pitchfork can simply be detected by the vanishing of the determinant of the Jacobian matrix. But in dynamic analysis using harmonic balance, this method does not apply unless we can foretell the newly born subharmonic terms and take them into consideration before the bifurcation occurs. For flip bifurcation, the number of terms used by Eq. (13) must be doubled to accommodate the period two subharmonics. Usually, the stability of the harmonic components can be examined using the determinant of the extended Jacobian matrix including the newly introduced subharmonic terms and the eigenvalues of the transition matrix in Floquet–Liapunov theory (Friedmann et al. 1977). The former is readily available in the Newton–Raphson iteration and the latter is discussed by Kim and Noah (1991) with the application of IFFT. The treatment is also useful in the present study because the Floquet eigenvalues can be deduced naturally from Eq. (9). Let $\mathbf{K}$ and $\bar{\mathbf{K}}$ represent the original Jacobian matrix in Eq. (33) and the extended Jacobian matrix in Eq. (34), respectively. If det[$\mathbf{K}$] and det[$\bar{\mathbf{K}}$] pass through zero while one of the eigenvalues increases through positive one, the point can be identified as a symmetry breaking or period one bifurcation. If det[$\mathbf{K}$] and det[$\bar{\mathbf{K}}$] pass through zero simultaneously while one of the eigenvalues decreases through negative one, the point can be identified as a period doubling bifurcation. If det[$\mathbf{K}$] passes through zero while the sign of det[$\bar{\mathbf{K}}$] remains unchanged, a fold point may be encountered with one of its eigenvalues growing through positive one.

## Dynamic Branch Switching

The associated eigenvalue problem of the extended Jacobian Matrix has to be solved in order to perform the branch switching from the first branch to the second. At bifurcation points, the Jacobian matrix [$\mathbf{K}$] is singular, the left and the right normal eigenvectors $\{\tilde{\phi}\}$ and $\{\tilde{\varphi}\}$ can be solved, respectively, by,

$$\begin{cases} \{\tilde{\phi}\}^T[\bar{\mathbf{K}}] = \{\mathbf{0}\}^T \\ [\bar{\mathbf{K}}]\{\tilde{\varphi}\} = \{\mathbf{0}\} \end{cases}. \tag{35}$$

If we define the solution on the branch $\mathbf{I}$ by $\{\mathbf{Y}_I\}$, the direction of this branch can be determined by

$$\{\vec{\mathbf{Y}}_\mathbf{I}\} = \frac{\partial\{\mathbf{Y}_\mathbf{I}\}}{\partial\rho}. \tag{36}$$

The direction on the second branch can be approximated by

$$\{\vec{\mathbf{Y}}_\mathbf{II}\} = \gamma\{\tilde{\varphi}\} + \{\vec{\mathbf{Y}}_\mathbf{I}\}, \tag{37}$$

where $\gamma = -2b/a$ (Riks, 1984), and $a$, $b$ are given as follows:

$$\begin{cases} a = \{\tilde{\phi}\}^T[\hat{\mathbf{K}}_\mathbf{X} \cdot \{\tilde{\varphi}\}]\{\tilde{\varphi}\} \\ b = \{\tilde{\phi}\}^T[\hat{\mathbf{K}}_\mathbf{X} \cdot \{\tilde{\varphi}\}]\{\vec{\mathbf{Y}}_\mathbf{I}\} \end{cases} \tag{38}$$

in which $\hat{\mathbf{K}}_\mathbf{X} = (\partial[\bar{\mathbf{K}}])/(\partial\{\mathbf{Y}\})$ is a tensor of rank 3. one may directly evaluate the matrix $[\hat{\mathbf{K}}_\mathbf{X} \cdot \{\tilde{\varphi}\}]$ instead of seeking the explicit form of $\hat{\mathbf{K}}_\mathbf{X}$.

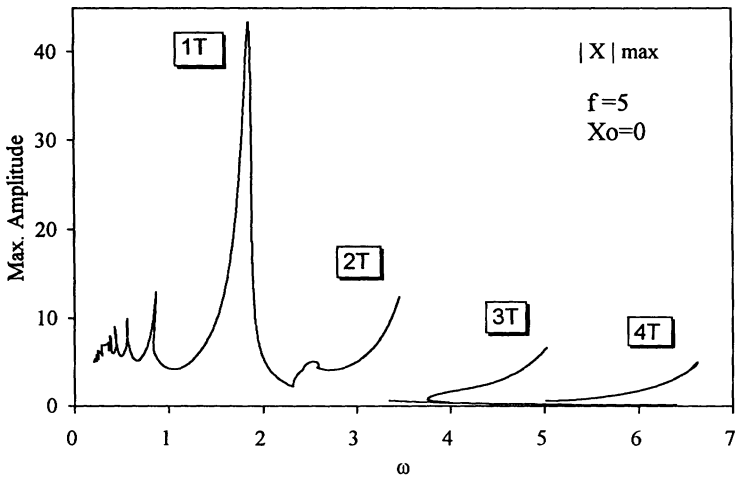


**FIGURE 5** Primary resonance and subharmonic resonances.

## STEADY-STATE SOLUTION AND BIFURCATION ANALYSIS

The frequency response of a system with step damping and piecewise-nonlinear stiffness function has been studied by the proposed method. As shown in Fig. 1, the system is bounded on the left side by a linear spring with a viscous damping, and on the right by a nonlinear spring with a viscous damping. A similar oscillator was studied by Shaw and Holmes (1983) and Shaw (1985). The configurations used in this example are $k_1 = 1$, $c_1 = 0.1$ and $k_2 = 10$, $c_2 = 0.05$, respectively. The amplitude of the sinusoidal excitation is taken as $P = 5$, and the initial gap length is assumed as $x_s = 0$. The overall frequency response of maximum amplitude within the frequency range from 0.2 to 7 obtained by augmentations along the solution curves in the frequency domain is shown in Fig. 5. The Floquet eigenvalues are computed together with augmentation to check the stability of the solutions. The branch switching techniques are performed at the flip bifurcation points to search for and to continue on the secondary stable branches. The subharmonic terms $\omega/n$ can be easily taken into the procedure by replacing the time transformations $\tau = \omega t$ with $\tau = n\omega t$, where $n$ refers to the order of the expected subharmonics. The complicated dynamic behaviors of the system including loops, fold, period doubled cascade, and Hopf bifurcation can be observed in the numerical computation. The primary resonance, the subharmonic resonance of period doubling, period tripling, and period quadrupling are investigated, respectively. The solution sought by the TJM/FFT method is accurately consistent with that given by numerical time integration. The number of the harmonic components $N$ is determined by the error tolerance given in the iteration. The smaller the required error tolerance is, the larger $N$ should be taken. Otherwise, the prediction of the equilibrium should be contaminated by the *mirror phenomenon* and results in a rapid divergence during its iteration process. The number of points for period discretization $M$ can be selected more flexibly in accordance with the impacting properties in damping and stiffness functions as well as the sampling theorem. Figure 6 shows the complex geometry of the period one solution curve provided by the method of TJM/FFT, where the heavy solid line represents the stable solutions and the fine line refers to the unstable ones. Superharmonic resonance is observed when the part of the high order components of response becomes eminent. Besides the sophisticated dynamic behavior shown at each equilibrium point [Fig. 7(a,b)], the stability of the solutions within this zone is weathered by the frequent occurrence of bifurcation points, such as fold bifurcation points and flip bifurcation points [Fig. 7(c,d)]. The locations of the bifurcation points can be accurately identified by the proposed method as shown in Table 1. In Fig. 8, the displacement response at time $2n\pi$ has been exhibited against the variation of the exciting frequency. At the point $\omega = 2.2832$ the period one solution loses its stability and bifurcates into period two. The period two solution bifurcates further into period four at the point $\omega = 2.4495$ and recovers its stability at $\omega = 2.5609$. At $\omega = 3.4567$ the period two subharmonic resonance occurs. The intermediate outputs of the phase diagram and the steady-state response of period four and

Table 1. List of the stability points in Fig. 6

| $\omega$ | $x_{max}$ | $\lambda$ | $\omega$ | $x_{max}$ | $\lambda$ | $\omega$ | $x_{max}$ | $\lambda$ |
|---|---|---|---|---|---|---|---|---|
| 0.232317 | 5.380729 | 1 | 0.357046 | 7.188346 | 1 | 0.563321 | 9.242371 | 1 |
| 0.238121 | 5.672891 | 1 | 0.356827 | 7.078709 | 1 | 0.556975 | 8.072759 | 1 |
| 0.243564 | 5.573986 | -1 | 0.377339 | 6.557063 | -1 | 0.657864 | 5.187241 | -1 |
| 0.253601 | 5.345887 | -1 | 0.386282 | 6.872217 | -1 | 0.707445 | 5.504688 | -1 |
| 0.254276 | 5.372999 | 1 | 0.390148 | 7.262276 | 1 | 0.861731 | 12.77275 | 1 |
| 0.257813 | 6.187421 | 1 | 0.378784 | 7.069842 | 1 | 0.837916 | 6.977158 | 1 |
| 0.261843 | 6.15499 | -1 | 0.413809 | 6.067374 | -1 | 0.972457 | 4.392126 | -1 |
| 0.287723 | 5.905029 | -1 | 0.436653 | 6.656034 | -1 | 1.083864 | 4.218935 | -1 |
| 0.293077 | 5.713127 | 1 | 0.443876 | 7.386998 | 1 | | | |
| 0.285395 | 6.936979 | 1 | 0.451062 | 6.698747 | 1 | | | |
| 0.290257 | 6.928102 | -1 | 0.497505 | 5.698065 | -1 | $\lambda = 1$ fold bif.pt. | | |
| 0.326664 | 6.996125 | -1 | 0.531597 | 6.302642 | -1 | $\lambda = -1$ flip bif. pt. | | |

period two solutions have been demonstrated, respectively, in Fig. 7 (e–h). The stability of the period one solution is regained at $\omega = 3.4441$ and remains unchanged up to the end. The Hopf bifurcation to period three can be found at $\omega = 3.9793$. At this point the bifurcated period three solution is unstable. Period three solution becomes stable at $\omega = 3.7760$ and proceeds along its upper branch up to the ultimate point at $\omega = 5.0258$ where the period three solution curve is folded back along the route closed together with the original one. A typical period three steady-state response and its phase diagram are shown in Fig. 7(i, j). Figure 9 exhibits the case when period one response and period three response coexist. Such diagrams are hard to acquire by the conventional time integration method. The period four Hopf bifurcation is found at the point $\omega = 5.5049$ and at $\omega = 6.6261$ the subharmonic resonance of period four is reached. A small loop can be seen near the resonant point. Similar to those discussed in the Hopf bifurcation of period three, it is found that the upper branch is stable while the lower branch is unstable. The steady-state responses and phase diagrams of a period four solution are shown in Fig. 7 (k–l). From the phase diagrams illustrated above we can see that the number of loops occurring on the phase curves is not equal to the orders of subharmonics in the nonlinear vibration, therefore, some naive identification techniques based on the loop counting should be used with caution.

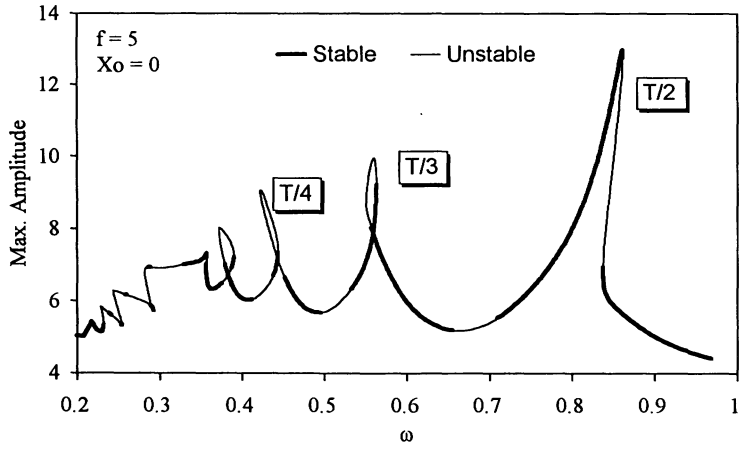


**FIGURE 6** Superharmonic resonances and bifurcations.

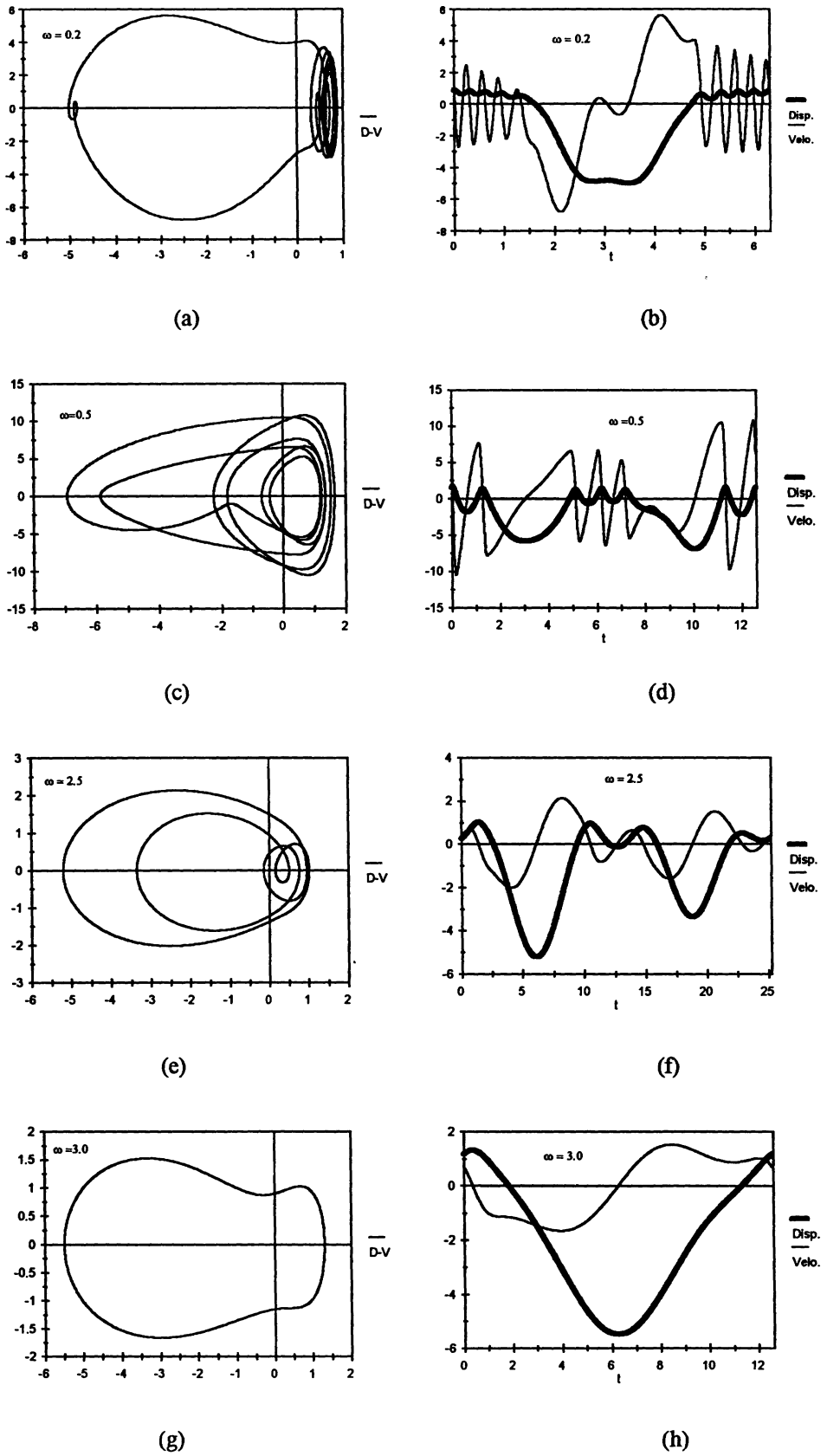


**FIGURE 7** Phase diagram and steady state responses.

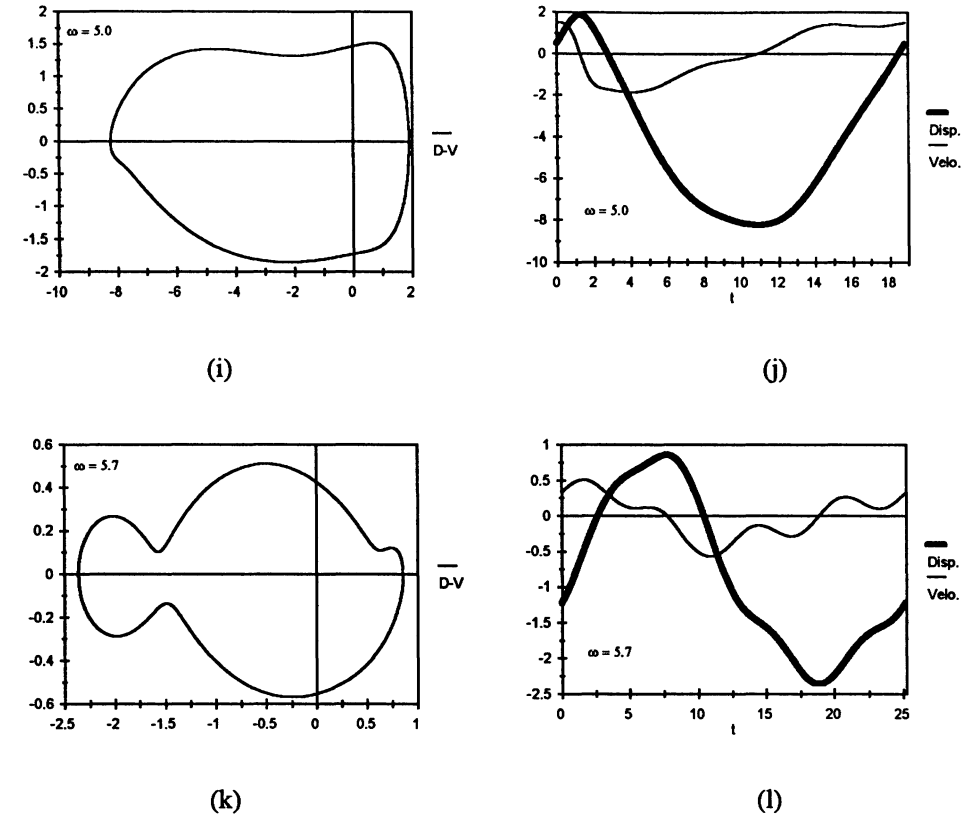


**FIGURE 7** *Continued*

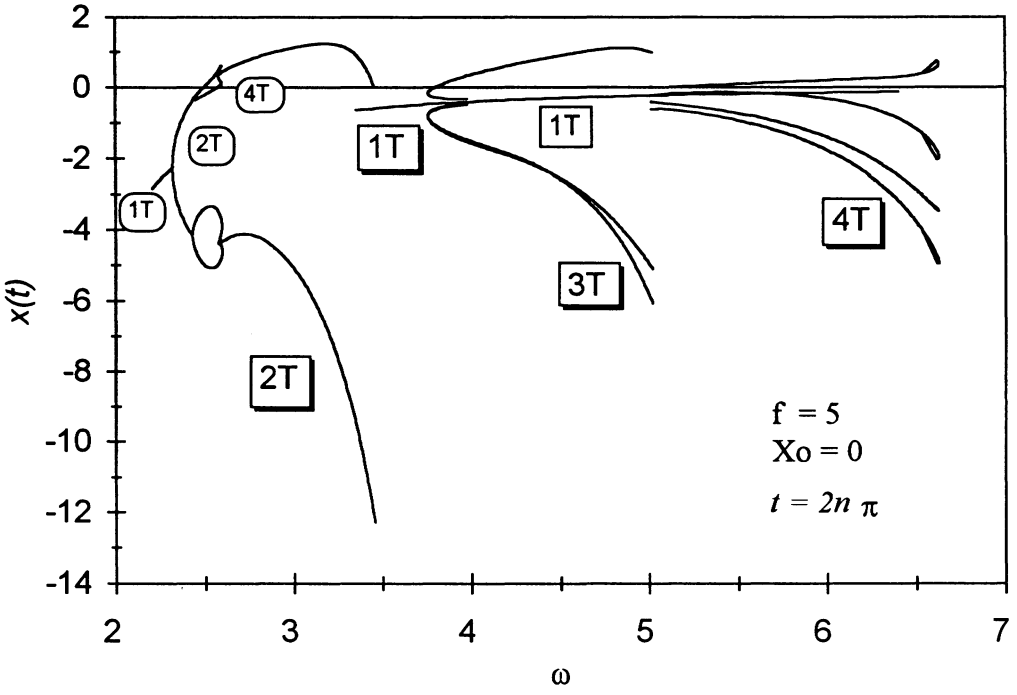


**FIGURE 8** A period double cascade and Hopf bifurcations.

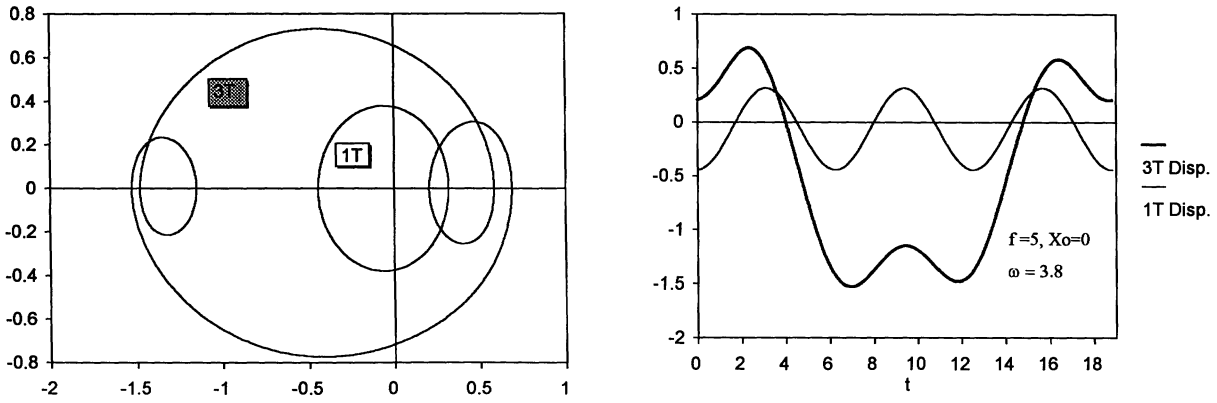


**FIGURE 9** Example for coexisted steady-state equilibriums.

## CONCLUSIONS

A new computational approach for steady-state analysis of oscillators with general piecewise nonlinearity has been proposed. The FFT/IFFT algorithm with a Toeplitz matrix is applied to determine the explicit form of the Jacobian matrix required by Newton–Raphson iterations. This leads to a renovated algorithm superior in the reduction of computational work, saving storage space as well as having the advantage of parallel computations. Leung and Ge (1993) have shown that the application of this method to the bifurcation analysis of a Duffing oscillator requires significantly less CPU time than the numerical time integration routines and even the incremental harmonic balance method. The TJM/FFT method also partly releases the collocated restriction on the sampling points between the time and the frequency domain. Thus it is possible to provide a more accurate approximation of response for a class of systems with general piecewise nonlinearity.

The frequency of a piecewise-nonlinear oscillator is investigated, and rich dynamic behaviors are observed. For period one resonance, the system response exhibits both fold and flip bifurcations as well as superharmonic resonance. Beyond the resonant frequency of period one, the system response shows the period two, the period three, and the period four subharmonic resonances that have been studied by many authors. A flip bifurcation with period double cascade and the Hopf bifurcations with isolated orbits have been demonstrated. Chaotic motions can be observed with some combination of system parameters but those phenomena are beyond the scope of the present study.

## REFERENCES

Bapat, C. N., and Sankar, S., 1986, "Exact Analysis of an Oscillator Hitting a Stop," *ASME Journal of Vibration, Acoustics, Stress, and Reliability in Design,* Vol. 107, pp. 347–350.

Brigham, E. O., 1974, *The Fast Fourier Transformation*, Prentice–Hall, New York.

Cameron, T. M., and Griffin, J. H., 1989, "An Alternating Frequency/Time Domain Method for Calculating the Steady-State Response of Nonlinear Dynamic Systems," *ASME Journal of Applied Mechanics,* Vol. 56, pp. 149–154.

Choi, Y. S., and Noah, S. T., 1988, "Forced Period Vibration of Unsymmetric Piecewise-Linear System," *Journal of Sound and Vibration,* Vol. 121, pp. 117–126.

Choi, Y. S., and Noah, S. T., 1989, "Periodic Response of a Link Coupling with Clearance," *ASME Journal of Dynamic Systems, Measurement and Control,* Vol. 111, pp. 253–259.

Comparin, R. J., and Singh, R., 1989, "Non-Linear Frequency Response Characteristics of an Impact Pair," *Journal of Sound and Vibration,* Vol. 134, pp. 259–290.

Crisfield, M. A., 1991, *Nonlinear Finite Element Analysis of Solids and Structures Volume 1: Essentials,* John Wiley & Sons, New York.

Ferri, A. A., 1986, "On the Equivalence of the Incremental Harmonic Balance Method and the Harmonic Balance Newton–Raphason Method," *ASME Journal of Applied Mechanics*, Vol. 53, pp. 455–457.

Friedmann, P., Hammond, C. E., and Woo, T. H., 1977, "Efficient Numerical Treatment of Periodic Systems with Application to Stability Problem," *International Journal for Numerical Methods in Engineering,* Vol. 11, pp. 1117–1136.

Kim, Y. B., and Noah, S. T., 1991, "Stability and Bifurcation Analysis of Oscillators with Piecewise-Linear Characteristics: A General Approach,"

*ASME Journal of Applied Mechanics*, Vol. 58, pp. 545–553.

Koh, C. G., and Liaw, C. Y., 1991, "Effect of Time Step Size on the Response of a Bilinear System, I: Numerical Study," *Journal of Sound and Vibration*, Vol. 144, pp. 17–29.

Lau, S. L., Cheung, Y. K., and Wu, S. Y., 1982, "Variable Parameter Incrementation Method for Dynamic Instability of Linear and Non-Linear System," *ASME Journal of Applied Mechanics*, Vol. 49, pp. 849–853.

Lau, S. L., and Zhang, W. S., 1992, "Nonlinear Vibrations of Piecewise-Linear Systems by Incremental Harmonic Balance Method," *ASME Journal of Applied Mechanics*, Vol. 59, pp. 153–160.

Leung, A. Y. T., and Fung, T. C., 1989, "Construction of Chaotic Regions," *Journal of Sound and Vibration*, Vol. 131, pp. 445–455.

Leung, A. Y. T., and Ge T., 1993. "Toeplitz Jacobian Matrix Method," to appear.

Ling, F. H., and Wu, X. X., 1987, "Fast Galerkin Method and Its Application to Determine Periodic Solutions of Nonlinear Oscillators," *International Journal of Nonlinear Mechanics*, Vol. 22, pp. 89–98.

Maezawa, S., and Furukawa, S., 1973, "Subharmonic Resonances in Piecewise-Linear System," *Bulletin of the JSME,* Vol. 16, pp. 931–941.

Masri, S. F., 1978, "Analytical and Experimental Studies of Dynamic System with a Gap," *ASME Journal of Mechanical Design,* Vol. 100, pp. 480–486.

Natsiavas, S., 1989, "Periodic Response and Stability of Oscillators with Symmetry Trilinear Restoring Force," *Journal of Sound and Vibration*, Vol. 134, pp. 315–331.

Nayfeh, A. H., and Mook, D. T., 1979, *Nonlinear Oscillations*, Wiley-Interscience, New York.

Pierre, C., Ferri, A. A., and Dowell, E. H., 1985, "Multi-Harmonic Analysis of Dry Function Damped Systems Using an Incremental Harmonic Balance Method," *ASME Journal of Applied Mechanics*, Vol. 52, pp. 958–964.

Riks, E., 1984, "Bifurcation and Stability, a Numerical Approach," in W. K. Lin et al., *Innovative Methods for Nonlinear Problems,* Pineridge Press, Swansea, pp. 313–345.

Shaw, S. W., and Holmes, P. J., 1983, "A Periodically Forced Piecewise Linear Oscillator," *Journal of Sound and Vibration,* Vol. 90, pp. 129–155.

Shaw, S. W., 1985, "Forced Vibration of a Beam with One-Sided Amplitude Constraint: Theory and Experiment," *Journal of Sound and Vibration*, Vol. 99, pp. 199–212.

Thompson, J. M. T., Bokaian, A. R., and Ghaffari, R., 1983, "Subharmonic Resonances and Chaotic Motions of a Bilinear Oscillator," *IMA Journal of Applied Mathematics*, Vol. 31, pp. 207–234.

Timoshenko, S. P., Young, D. H., and Weaver, W. Jr., 1974, *Vibration Problems in Engineering,* 4th ed., John Wiley & Sons, New York.

Urabe, M., 1965, "Galerkin's Procedure for Nonlinear Periodic Systems," *Archives of Rat. Mech. Anal.*, Vol. 20, pp. 120–152.